Atom-atom interaction in strongly modified reservoirs

Søren Bay,[1,2] P. Lambropoulos,[2,3] and Klaus Mølmer[1]
[1]*Institute of Physics and Astronomy, University of Aarhus, 8000 Aarhus C, Denmark*
[2]*Max-Planck-Institut für Quantenoptik, Hans-Kopfermann-Strasse 1, 85748 Garching, Germany*
[3]*Institute of Electronic Structure and Laser, FORTH, P.O. Box 1527, Heraklion 71110, Crete, Greece and Department of Physics, University of Crete, Crete, Greece*
(Received 26 June 1996)

We extend recent work on two closely spaced atoms interacting through the narrow band of strongly coupled modes at the edge of a photonic band gap. The resonant dipole-dipole interaction (RDDI) is strongly modified for atomic transition frequencies in the vicinity of the band-gap edge, but we show that an analytical approximation to the RDDI agrees very well with the exact RDDI obtained by numerical integration using the exact dispersion relation. Having established the value of the RDDI, we can derive the amplitudes for the two atoms without resorting to the pole approximation which is necessary due to the strongly modified mode structure in the dielectric host. For a wide range of parameters we find beating and population trapping in the long time limit. The distribution of population in the photonic continuum is investigated in the long time limit in the case of one and two atoms. It is found to be strongly asymmetric and to exhibit a strong signature of the unusual mode structure in the material at the band-gap edge. [S1050-2947(97)05902-7]

PACS number(s): 42.50.Lc, 42.70.Qs, 42.50.Md

I. INTRODUCTION

The behavior of a two-level atom in a modified radiation reservoir, such as a high-quality cavity, has become the standard testing ground for novel effects of quantum electrodynamics (QED) and has revealed a number of striking features. For instance, the spontaneous exponential decay of an excited atomic state in free space, traditionally thought of as an inherent property of the atom, can be enhanced or suppressed by enclosing the atom in a near-resonant cavity, depending on the magnitude of the atomic lifetime in vacuum relative to the lifetime of the photons in the cavity mode.

The recent emergence of materials with photonic band gaps has given rise to a new direction of inquiry, namely, the behavior of atomic decay inside such materials. By conception and construction, the periodic modulation of the dielectric constant in these materials leads to a strongly modified mode structure such that photonic modes do not exist for a continuous range of frequencies that can be much larger than a typical atomic linewidth.

For an atom with transition frequency in the band gap and located inside the dielectric host, this may lead to a total inhibition of spontaneous decay [1], which in turn yields a so-called photon-atom bound state [2] in which the radiation remains localized at the atom. For atomic transition frequencies closer to the band-gap edge, the rapidly varying density of modes leads to a splitting of the atomic level, which in the time domain yields the rather unusual phenomenon of an oscillatory spontaneous decay [3,4].

In parallel and independent developments, the issue of the modification of atomic radiative behavior under atom-atom resonant dipole-dipole interaction (RDDI) has been receiving renewed attention. Beginning with the pioneering Dicke paper on super-radiance [5,6], the interaction of two closely spaced atoms sharing a photon in open space has been addressed in numerous studies, with the prediction of interesting effects such as atomic level shifts due to RDDI, oscillatory photon exchange and squeezing of two-atom resonance fluorescence. And rather recently a natural generalization of these phenomena has been addressed, namely, the study of the RDDI of closely spaced atoms inside a near-resonant perfect cavity [7]. The results predict a rather strong competition between RDDI and the atom-cavity coupling in the limit of small interatomic separations such that these two couplings become comparable in magnitude.

These developments point to two further levels of generalization. First, the interplay between RDDI and atom-cavity coupling in an open (lossy) cavity and, second, the same interplay with the cavity replaced by a photonic band-gap environment. It is precisely these generalizations that we have undertaken in this paper thus extending recent work [8]. We have thus addressed the problem of two identical two-level atoms with a transition frequency in the vicinity of the band-gap edge and interacting through the narrow band of strongly coupled modes. This gives rise to many new effects and since it is important to distinguish the effects stemming from the modified mode structure from those coming from the interatomic interaction, we have contrasted the results with known results for atoms in free space as well as two atoms coupled to a lossy cavity which we have obtained here.

The dynamics of a collection of two-level atoms with transition frequencies far inside the gap has been investigated by John and Quang [9]. In that case, the spontaneous decay is strongly suppressed but the RDDI between the atoms remains strong.

In addition to the theoretical interest in these questions, technological developments are making them accessible to experiment. Although the appropriate photonic band-gap materials are not yet available in the optical regime, effects stemming from atom-atom coupling in an open cavity have already been observed [10].

This paper is organized as follows: In the next section we present the model. In Sec. III we calculate the couplings

entering the equations of motion, which allows us to solve these equations in Sec. IV. The inversion is performed in Sec. V and the dynamics is investigated in time domain in Sec. VI. In Sec. VII we calculate the distribution of population in the photonic continuum in the long time limit.

II. MODEL

We consider two two-level atoms situated at different locations $\mathbf{R}_A, \mathbf{R}_B$ in space. Taking $\hbar = 1$, the second quantized Hamiltonian for the problem under consideration reads

$$H = H_0 + V \tag{2.1}$$

with

$$H_0 = \omega_A \sigma_A^z + \omega_B \sigma_B^z + \sum_{\mathbf{k}} \omega_{\mathbf{k}} a_{\mathbf{k}}^\dagger a_{\mathbf{k}} \tag{2.2}$$

neglecting the zero-point energy of the field modes, and

$$V = i \sum_{\mathbf{k}} g_{\mathbf{k}} [a_{\mathbf{k}} e^{i\mathbf{k}\cdot\mathbf{R}_A} \sigma_A^+ - a_{\mathbf{k}}^\dagger e^{-i\mathbf{k}\cdot\mathbf{R}_A} \sigma_A^-] + i \sum_{\mathbf{k}} g_{\mathbf{k}} [a_{\mathbf{k}} e^{i\mathbf{k}\cdot\mathbf{R}_B} \sigma_B^+ - a_{\mathbf{k}}^\dagger e^{-i\mathbf{k}\cdot\mathbf{R}_B} \sigma_B^-], \tag{2.3}$$

which is the ordinary interaction Hamiltonian in the rotating wave approximation where $\sigma^+, \sigma^-, \sigma^z$ are the atomic operators and $a_{\mathbf{k}}^\dagger, a_{\mathbf{k}}$ are the creation and annihilation operators of the vacuum modes, respectively, and the dependence on the atomic positions $\mathbf{R}_A, \mathbf{R}_B$ is shown explicitly. The coupling constant is given by

$$g_{\mathbf{k}} = \sqrt{\frac{\omega_{\mathbf{k}}}{2\varepsilon_0 V}} \mathbf{e}_{\mathbf{k}} \cdot \mathbf{d}_{ij}. \tag{2.4}$$

Here $\mathbf{d}_{ij}$ is the atomic dipole moment, V the quantization volume, $\mathbf{e}_{\mathbf{k}}$ the polarization vector, and $\omega_{\mathbf{k}}$ the photon energy.

The relevant states of the problem are

$$a = |e_A, g_B, 0\rangle,$$

$$b = |g_A, e_B, 0\rangle,$$

$$c = |g_A, g_B, 1_{\mathbf{k}e_l}\rangle, \tag{2.5}$$

where $g_{A(B)}, e_{A(B)}$ denote lower and upper states of the atoms $A(B)$, respectively, and the states c represent the photonic continuum.

As a means of deriving the appropriate equations for the atom-field dynamics nonperturbatively, we employ the resolvent operator [11],

$$G(z) = \frac{1}{z - H}, \tag{2.6}$$

which is the Laplace transform of the time-evolution operator, with z being the complex transform variable and H the full Hamiltonian of the system. This formalism, in terms of the wave functions instead of the density operator, is applicable here since we have no incoherent pumping of the system under consideration and we do not perform a trace over the vacuum field modes.

With the system initially in state a, the matrix elements of the resolvent operator read

$$(z - \omega_a) G_{aa} = 1 + \sum_c V_{ac} G_{ca},$$

$$(z - \omega_b) G_{ba} = \sum_c V_{bc} G_{ca},$$

$$(z - \omega_c) G_{ca} = V_{cb} G_{ba} + V_{ca} G_{aa}.$$

Eliminating the continuum amplitude G_{ca}, we find the two coupled algebraic equations

$$(z - \omega_a) G_{aa} = 1 + \sum_c \frac{|V_{ac}|^2}{z - \omega_c} G_{aa} + \sum_c \frac{V_{ac} V_{cb}}{z - \omega_c} G_{ba}, \tag{2.7}$$

$$(z - \omega_b) G_{ba} = \sum_c \frac{|V_{bc}|^2}{z - \omega_c} G_{ba} + \sum_c \frac{V_{bc} V_{ca}}{z - \omega_c} G_{aa} \tag{2.8}$$

containing several couplings, one of which is

$$\sum_c \frac{|V_{ac}|^2}{z - \omega_c} \tag{2.9}$$

describing the emission of a photon by atom A followed by a propagation of all the modes, before the photon is eventually reabsorbed by atom A.

Up to this point we have made no approximations specific to a band-gap material and the two equations above could therefore as well describe two atoms in the vacuum of free space. The propagation of photons in a band-gap material is strongly modified and it is therefore natural to expect a modification of the couplings, which will indeed be the case, as we show in the next section. But before proceeding to this issue, let us for instructive purposes investigate the cases of two atoms first in vacuum and second in an open cavity.

A. Atom-atom interaction in free space vacuum

In this case we can perform the usual pole approximation in the couplings which consists in replacing the Laplace variable z by the atomic transition frequency ω_A. The justification for performing this approximation is that the free space continuum (vacuum) is flat and changing the Laplace variable z around ω_A does not change the value of the coupling significantly. In the pole approximation the couplings yield

$$\sum_c \frac{|V_{ac}|^2}{z - \omega_c} \simeq \Delta - i\Gamma, \tag{2.10}$$

$$\sum_c \frac{|V_{bc}|^2}{z - \omega_c} \simeq \Delta - i\Gamma, \tag{2.11}$$

$$\sum_c \frac{V_{ac} V_{cb}}{z - \omega_c} \simeq M_{ab}, \tag{2.12}$$

assuming identical atoms and thus identical shifts and widths. The dipole-dipole matrix element M_{ab} is in general complex and diverges when the interatomic distance R goes to zero. This formal divergence stems from the fact that our model does not allow for molecule formation as the atoms approach each other and for our purposes, we do not need to allow for that case.

Inserting these quantities in the equations for the resolvent operator and writing these in matrix form, we find

$$\begin{bmatrix} z-\tilde{\omega}+i\Gamma & -M_{ab} \\ -M_{ba} & z-\tilde{\omega}+i\Gamma \end{bmatrix}\begin{bmatrix} G_{aa} \\ G_{ba} \end{bmatrix}=\begin{bmatrix} 1 \\ 0 \end{bmatrix}, \tag{2.13}$$

where the shift has been absorbed in $\tilde{\omega}$.

The eigenvalues, which are easily found as

$$z_{\pm}=\tilde{\omega}-i\Gamma\pm M_{ab}, \tag{2.14}$$

lead to a damped sinusoidal dynamics in the time domain. Whether the damping or the sinusoidal behavior is dominant depends on the strength of M_{ab}, which in turn is determined by the atomic configuration and separation. In the long time limit and for finite separations there is no population trapping.

B. Atom-atom interaction in a cavity

Equations (2.7) and (2.8) are easily extended to accommodate the presence of an open cavity

$$(z-\omega_a)G_{aa}=1+\sum_c \frac{|V_{ac}|^2}{z-\omega_c}G_{aa}+\sum_c \frac{V_{ac}V_{cb}}{z-\omega_c}G_{ba} + \frac{|V_{ad}|^2}{z-\tilde{\omega}_d+i\kappa}G_{aa}+\frac{V_{ad}V_{db}}{z-\tilde{\omega}_d+i\kappa}G_{ba}, \tag{2.15}$$

$$(z-\omega_b)G_{ba}=\sum_c \frac{|V_{bc}|^2}{z-\omega_c}G_{ba}+\sum_c \frac{V_{bc}V_{ca}}{z-\omega_c}G_{aa} + \frac{|V_{bd}|^2}{z-\tilde{\omega}_d+i\kappa}G_{ba}+\frac{V_{bd}V_{da}}{z-\tilde{\omega}_d+i\kappa}G_{aa}, \tag{2.16}$$

where V_{ad}, (V_{bd}) are the dipole-mode couplings of atom A (B), respectively, $\tilde{\omega}_d$ is the resonance frequency of the cavity shifted due to the coupling to a reservoir, and κ the cavity decay width. These equations show that the presence of the cavity can be thought of as a Lorentzian superimposed on the flat background of vacuum modes.

Since the summations in the couplings are over the flat continuum (vacuum), we perform the pole approximation as in Eqs. (2.10)–(2.12) and bring the equations to the matrix form

$$\begin{bmatrix} z-\tilde{\omega}+i\Gamma-\dfrac{|V_{ad}|^2}{z-\tilde{\omega}_d+i\kappa} & -M_{ab}-\dfrac{V_{ad}V_{db}}{z-\tilde{\omega}_d+i\kappa} \\ -M_{ba}-\dfrac{V_{bd}V_{da}}{z-\tilde{\omega}_d+i\kappa} & z-\tilde{\omega}+i\Gamma-\dfrac{|V_{bd}|^2}{z-\tilde{\omega}_d+i\kappa} \end{bmatrix}\begin{bmatrix} G_{aa} \\ G_{ba} \end{bmatrix} =\begin{bmatrix} 1 \\ 0 \end{bmatrix}. \tag{2.17}$$

The motion of the coupled system is determined by the poles of the resolvent operator which are the roots of the characteristic polynomial.

In general, all three roots are complex and thus contain dissipative terms. This means that in the long time limit $t\gg\Gamma^{-1},\kappa^{-1}$, there will be no population trapping as opposed to two atoms located in a photonic band-gap material, which is the case we treat in the rest of this paper.

III. CALCULATION OF THE COUPLINGS

As a model for the photonic band-gap material, we consider the isotropic crystal introduced by John [12], for which the dispersion relation can be found analytically as

$$\omega_k=\frac{c}{4na}\arccos\left[\frac{4n\,\cos(kL)+(1-n)^2}{(1+n)^2}\right], \tag{3.1}$$

where c is the speed of light and n, L, and a are constants pertaining to the crystal. The dispersion relation (3.1) exhibits gaps in frequency at the spheres $k=m\pi/L$ with $m=1,2,\ldots$. In the following we choose the refractive index $n=1.082$, which yields a gap center frequency $\omega_0=(\pi c/L)[(1+n)/2n]$ and a relative gap width $\Delta\omega/\omega_0=0.05$. At (near-)optical frequencies, this gap is much larger than any typical atomic coupling and the influence of the lower band-gap edge on the atomic dynamics can therefore be neglected for atomic transition frequencies in the vicinity of the upper band edge.

The assumption underlying Eq. (3.1) is that photons propagating in the photonic band-gap material experience the same mode structure for both polarizations and in all spatial directions. Close to the band edge, the dispersion relation (3.1) can be approximated by the effective mass dispersion relation [12]

$$\omega_k\simeq\omega_e+A(k-k_0)^2, \tag{3.2}$$

where k_0 is the wave vector corresponding to the band-edge frequency and A is given by

$$A=\frac{-cL^2}{2a(1+n)^2}\frac{1}{\sin(4na\omega_e/c)} \tag{3.3}$$

containing constants only pertaining to the structure of the crystal.

In this section we address the calculation of the couplings

$$\sum_c \frac{V_{mc}V_{cn}}{z-\omega_c} \tag{3.4}$$

with $m,n\in\{a,b\}$ which when using the interaction Hamiltonian (2.3) can be written more explicitly as

$$\sum_c \frac{V_{mc}V_{cn}}{z-\omega_c} = \sum_{\mathbf{k},i,j,l} \frac{\omega_\mathbf{k}}{2\varepsilon_0 V} \frac{(e^{(l)}_{\mathbf{k}i} d^m_{egi}) e^{(l)}_{\mathbf{k}j} d^n_{gej}}{z-\omega_c} e^{i\mathbf{k}\cdot\mathbf{R}} \quad (3.5)$$

with $\mathbf{R}=\mathbf{R}_m-\mathbf{R}_n$ the relative distance between the two atoms if $m\neq n$, $i,j\in\{x,y,z\}$ and we have introduced a summation over polarization (index l) in the first equation. It is easily shown that the summation over polarization vectors yields

$$\sum_{l=1,2} e^{(l)}_{\mathbf{k}i} e^{(l)}_{\mathbf{k}j} = \delta_{ij} - \hat{k}_i \hat{k}_j \quad (3.6)$$

where $\hat{\mathbf{k}}=(\sin\theta\cos\phi,\sin\theta\sin\phi,\cos\theta)$. Inserting this relation in the expression above and turning the summation over $\mathbf{k}$ into an integral, the relation reads

$$\sum_c \frac{V_{mc}V_{cn}}{z-\omega_c} = \frac{1}{(2\pi)^3}\sum_{ij} \int d^3k (\delta_{ij}-\hat{k}_i\hat{k}_j) \times \frac{\omega_\mathbf{k}}{2\varepsilon_0} \frac{d^m_{egi} d^n_{gej}}{z-\omega_\mathbf{k}} e^{i\mathbf{k}\cdot\mathbf{R}}. \quad (3.7)$$

Since we have assumed an isotropic dispersion relation which contains no angular dependence, the angular integral can thus be performed.

The general result reads

$$\sum_c \frac{V_{mc}V_{cn}}{z-\omega_c} = \frac{1}{2\pi^2}\frac{1}{2\varepsilon_0}\sum_i \int dk k^2 \omega_k \tau_{ii}(k,R) \frac{d^m_{egi} d^n_{gei}}{z-\omega_k} \quad (3.8)$$

with

$$\tau_{ii}(k,R) = \left[\frac{\sin kR}{kR} + \frac{\cos kR}{(kR)^2} - \frac{\sin kR}{(kR)^3}\right]\delta_{ix} + \left[\frac{\sin kR}{kR} + \frac{\cos kR}{(kR)^2} - \frac{\sin kR}{(kR)^3}\right]\delta_{iy} + \left[-\frac{2\cos kR}{(kR)^2} + \frac{2\sin kR}{(kR)^3}\right]\delta_{iz}, \quad (3.9)$$

where we have taken the z axis along the interatomic separation axis.

The steps leading to Eq. (3.8) are standard and well known. For $m\neq n$, Eq. (3.8) yields the RDDI between two neighboring atoms and for $m=n$ the effective coupling of an atom with the reservoir. In that case $R=0$.

For two atoms in free space, the free space dispersion relation $\omega_k=ck$ applies and the integral (3.8) can be evaluated by contour methods yielding the matrix element M_{ab} of Eqs. (2.14) and (2.17). In the present context, the dispersion relation (3.1) is rather complicated and the integral (3.8) has to be performed numerically.

The question of major interest here is whether we can replace the variable z by the atomic transition energy ω_A in Eq. (3.8). This requires that the integral as a function of z is slowly varying. Calculations by John [12] and Kweon [13] have shown that for atomic transition frequencies in the gap far from the edge, the value of the dipole-dipole matrix element approaches that of vacuum, i.e., for two closely spaced atoms with transition frequencies in the gap, the virtual photons exchanged are of such energy that the atoms do not experience the existence of the gap. It is, however, not evident whether this also holds for atomic transition frequencies at the edge of the gap. To explore the sensitivity of the value of the integral on z, we have performed a careful numerical investigation of the coupling (3.8) using the exact dispersion relation (3.1) for the crystal and have indeed found that the value Eq. (3.8) assumes in the vicinity of the band edge is sensitively dependent on z and as a result we cannot replace z by ω_A.

Before proceeding to the numerical results, we present an approximate analytical calculation of the coupling. The complex Laplace variable z can in this context be written $z=x+i\eta$, where η is a small positive quantity. Using the identity

$$\frac{1}{x+i\eta} \overset{\eta\to 0}{=} \mathcal{P}\frac{1}{x} - i\pi\delta(x) \quad (3.10)$$

where $\mathcal{P}$ denotes principal value part, in the integral (3.8) and leaving out for the moment the multiplicative coefficients yields

$$\int dk k^2 \omega_k \tau_{ii}(k,R) \frac{1}{z-\omega_k} = \mathcal{P}\int dk k^2 \omega_k \tau_{ii}(k,R) \frac{1}{x-\omega_k} - i\pi \int dk k^2 \omega_k \tau_{ii}(k,R) \times \delta(x-\omega_k). \quad (3.11)$$

For $m\neq n$, we denote the first part of Eq. (3.11) by V_{mn} and this gives rise to the divergent part of the dipole-dipole interaction, diverging for small interatomic distances as $1/R^3$. By numerical integration of this quantity, we have established that it is to a very good approximation given by the real part of the RDDI obtained for two atoms in free space.

For $m=n$ the principal value part gives rise to the Lamb shift of the excited atomic states. We absorb this energy shift in the eigenenergies of the excited atomic states. To evaluate the second integral of Eq. (3.11), we apply the effective-mass approximation (3.2). Inserting this expression in the integral (3.11) yields

$$\int dk k^2 \omega_k \tau_{ii}(k,R)\delta(x-\omega_k) \simeq k_+^2 \omega_{k_+} \tau_{ii}(k_+,R) \frac{1}{2\sqrt{x-\omega_e}\sqrt{A}} \quad (3.12)$$

where $k_+=k_0+\sqrt{(x-\omega_e)/A}$.

For atomic transition frequencies at the edge of the gap $\omega_A\simeq\omega_e$, the contribution $\sqrt{(x-\omega_e)/A}$ will be negligible since the resolvent operator has a pole at $x\simeq\omega_A\simeq\omega_e$. Neglecting $\sqrt{(x-\omega_e)/A}$ compared to k_0, we thus find the simpler expression

$$\int dk k^2 \omega_k \tau_{ii}(k,R)\delta(x-\omega_k) \simeq k_0^2 \omega_e \tau_{ii}(k_0,R) \frac{1}{2\sqrt{x-\omega_e}\sqrt{A}}, \quad (3.13)$$

which applies to the case of $m=n$ as well as $m\neq n$.

For notational convenience, we define

$$C_M=\sum_i \frac{1}{4\pi\epsilon_0}\frac{d^m_{egi}d^n_{gei}}{2\sqrt{A}}k_0^2\omega_e\tau_{ii}(k_0,R) \tag{3.14}$$

for $m\neq n$ and

$$C_n=\sum_i \frac{1}{4\pi\epsilon_0}\frac{|d^n_{egi}|^2}{2\sqrt{A}}k_0^2\omega_e\tau_{ii}(k_0,R=0)$$

$$=\sum_i \frac{1}{4\pi\epsilon_0}\frac{|d^n_{egi}|^2}{2\sqrt{A}}k_0^2\omega_e\frac{2}{3} \tag{3.15}$$

for $m=n$.

In the Σ configuration, for instance, i.e., the atomic dipoles parallel and aligned perpendicular to the interatomic separation axis, C_M reads

$$C_M=\frac{\omega_e}{4\pi\epsilon_0}\frac{d^m_{eg}d^n_{ge}}{2\sqrt{A}}\left[\frac{k_0\sin k_0R}{R}+\frac{\cos k_0R}{R^2}-\frac{\sin k_0R}{k_0R^3}\right]. \tag{3.16}$$

Collecting the terms, we find

$$\sum_c \frac{|V_{ac}|^2}{z-\omega_c}=\frac{-iC_a}{\sqrt{z-\omega_e}}, \tag{3.17}$$

where the Lamb shift part of the coupling has been absorbed in the atomic eigenenergies and

$$\sum_c \frac{V_{ac}V_{cb}}{z-\omega_c}=V_{ab}+\frac{-iC_M}{\sqrt{z-\omega_e}}, \tag{3.18}$$

where V_{ab} is the principal value part of the RDDI integral in Eq. (3.11). We note that the RDDI (3.18) has a term diverging as $z\rightarrow\omega_e$. For atomic transition frequencies outside the gap, i.e., $z>\omega_e$, this yields an imaginary contribution to the interatomic coupling. For atomic transition frequencies in the gap, i.e., $z<\omega_e$, the argument of the square root changes sign and the square root term and thus the whole interatomic coupling becomes purely real. As has been noted in the literature [12], the occurrence of the square root terms in Eqs. (3.18) and (3.17) corresponds to a density of states given by

$$\rho(\omega)=\frac{V}{(2\pi)^3}\frac{k_0^2}{2\sqrt{A}}\frac{1}{\sqrt{\omega-\omega_e}}\Theta(\omega-\omega_e), \tag{3.19}$$

where $\Theta(\omega-\omega_e)$ is the Heaviside step function. The divergence of the density of states at the band edge is an artifact and stems from the assumption of an isotropic dispersion relation, i.e., a spherical crystal. A real photonic crystal will in general have a spatial anisotropy which in turn will be reflected in the dispersion relation. In the following, we assume V_{ab} and C_M to be real quantities, which is not a restriction, since this can be achieved by a proper phase transformation of the interaction Hamiltonian turning the dipole moments into real quantities.

To check the validity of the effective-mass approximation in calculating the RDDI, we present the results obtained from Eq. (3.18) and by numerical integration of Eq. (3.8). In Fig. 1, we compare the results obtained by numerical integration of the exact expression for the coupling (3.8) with the approximate analytical result (3.18) obtained in the effective-mass approximation as a function of the interatomic separation with $z=0.998\omega_e$. As the real part of the RDDI of Eq. (3.18) we have used the coupling obtained for two atoms in vacuum. There is indeed a very good agreement. For this choice of parameters, $z<\omega_e$ which yields a negative argument in the square root part of Eq. (3.18) and the coupling is thus purely real.

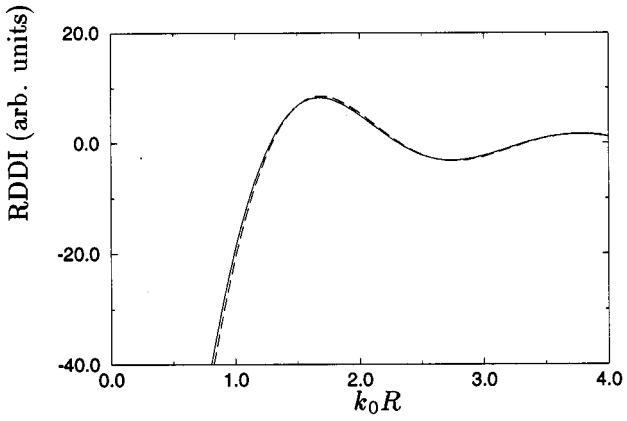

FIG. 1. RDDI as a function of the interatomic distance R for atoms in the Σ configuration with $z=0.998\omega_e$. The solid line is the numerical solution of Eq. (3.8) and the dotted curve that of Eq. (3.18).

In Fig. 2, we plot the coupling with $z=1.002\omega_e$. Again we find a very good agreement between the exact expression (3.8) and the approximate expression (3.18). We have tested the sensitivity of Eq. (3.8) on z by calculating the coupling for various values of z in the vicinity of ω_e and the dependence on z as given by the approximate expression in Eq. (3.18) has been confirmed. We have thus shown that the RDDI given by Eq. (3.8) can be replaced by the more ex-

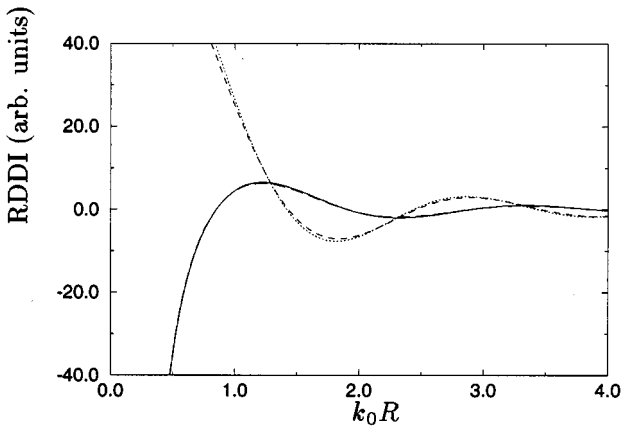

FIG. 2. RDDI as a function of the interatomic distance R for atoms in the Σ configuration with $z=1.002\omega_e$. The solid and long-dashed lines are the numerical computations of Eqs. (3.8) and (3.18), respectively. The dotted and dashed lines are the imaginary parts of Eqs. (3.8) and (3.18), respectively.

plicit expression (3.18), where V_{ab} is the real part of the dipole-dipole coupling for two atoms in the vacuum of free space.

IV. REVISITING THE RESOLVENT OPERATOR EQUATIONS

Using Eqs. (3.17) and (3.18) in the equation for the resolvent matrix elements, we find

$$(z-\omega_a)G_{aa}=1+V_{ab}G_{ba}+\frac{-iC_a}{\sqrt{z-\omega_e}}G_{aa}+\frac{-iC_M}{\sqrt{z-\omega_e}}G_{ba},$$

$$(z-\omega_b)G_{ba}=V_{ba}G_{aa}+\frac{-iC_b}{\sqrt{z-\omega_e}}G_{ba}+\frac{-iC_M}{\sqrt{z-\omega_e}}G_{aa},$$

assuming as before that the matrix element C_M is real. The equations can be slightly simplified by multiplying both sides of the equations with $\sqrt{z-\omega_e}$ and transforming the Laplace variable z by $z-\omega_a\rightarrow z$, which corresponds to transforming to an interaction picture rotating at ω_a. We further assume $\omega_a=\omega_b$ and $C_a=C_b\equiv C$, i.e., the atoms are identical and define $\delta=\omega_a-\omega_e$.

Writing the equations in matrix form finally yields

$$\begin{bmatrix} z\sqrt{z+\delta}+iC & -\sqrt{z+\delta}V_{ab}+iC_M \\ -V_{ba}\sqrt{z+\delta}+iC_M & z\sqrt{z+\delta}+iC \end{bmatrix}\begin{bmatrix} G_{aa} \\ G_{ba} \end{bmatrix} =\begin{bmatrix} \sqrt{z+\delta} \\ 0 \end{bmatrix}. \tag{4.1}$$

Eliminating the continuum amplitude, we have obtained two coupled algebraic equations for two two-level atoms interacting through RDDI and through a narrow band of strongly coupled modes. As opposed to standard treatments dealing with system-reservoir interactions, we have at no point performed a pole-approximation simply because the reservoir in our case is very far from being ''flat.'' The peculiar features of the continuum are reflected by the square root terms appearing in the resolvent operator equations.

We can immediately identify the eigenstates of the matrix in Eq. (4.1) as the symmetric and antisymmetric product states defined by

$$\psi_{s(a)}=\frac{1}{\sqrt{2}}[|e_Ag_B\rangle\pm|g_Ae_B\rangle]. \tag{4.2}$$

The symmetric product state ψ_s is a Dicke state and would for atoms in free space correspond to a superradiant state. We shall, however, see that in a photonic band-gap material we can actually have population trapping in this symmetric state.

In the study of the interactions of atoms with cavity modes, the dynamics of the systems under consideration is exclusively determined by the location of the poles of the resolvent operator in the complex plane. This is, however, not the full truth in this problem; on performing the inversion integral to obtain the time dependent amplitudes, there is a contribution coming from the cut in the complex plane (arising from the photonic continuum) which yields a non-negligible contribution to the dynamics of the system. But for the moment, we proceed as usual by finding the roots of the characteristic polynomial of the above equations. It reads

$$0=[z\sqrt{z+\delta}+iC]^2-[\sqrt{z+\delta}V_{ab}-iC_M]^2 \tag{4.3}$$

assuming that V_{ab} is real. To obtain a polynomial in z, we multiply by the conjugate, which yields the characteristic polynomial

$$h(z)=[z^2(z+\delta)-C^2-V_{ab}^2(z+\delta)+C_M^2]^2 +4(z+\delta)[Cz+C_MV_{ab}]^2. \tag{4.4}$$

By multiplying the characteristic equation with its conjugate, we have of course introduced extra roots and thereby extra poles. These extra poles, however, do not contribute when we perform the inversion integral.

In general, the roots of Eq. (4.4) are complicated expressions and they read

$$z_1=\frac{-\delta-2V_{ab}}{3}+\frac{2^{1/3}(\delta-V_{ab})^2}{3B_-}+\frac{B_-}{3\times 2^{1/3}}, \tag{4.5}$$

$$z_2=\frac{-\delta-2V_{ab}}{3}-e^{i\pi/3}\frac{2^{1/3}(\delta-V_{ab})^2}{3B_-}-e^{-i(\pi/3)}\frac{B_-}{3\times 2^{1/3}}, \tag{4.6}$$

$$z_3=\frac{-\delta-2V_{ab}}{3}-e^{-i\pi/3}\frac{2^{1/3}(\delta-V_{ab})^2}{3B_-}-e^{i(\pi/3)}\frac{B_-}{3\times 2^{1/3}}, \tag{4.7}$$

$$z_4=\frac{-\delta+2V_{ab}}{3}+\frac{2^{1/3}(\delta+V_{ab})^2}{3B_+}+\frac{B_+}{3\times 2^{1/3}}, \tag{4.8}$$

$$z_5=\frac{-\delta+2V_{ab}}{3}-e^{i\pi/3}\frac{2^{1/3}(\delta+V_{ab})^2}{3B_+}-e^{-i(\pi/3)}\frac{B_+}{3\times 2^{1/3}}, \tag{4.9}$$

$$z_6=\frac{-\delta+2V_{ab}}{3}-e^{-i\pi/3}\frac{2^{1/3}(\delta+V_{ab})^2}{3B_+}-e^{i(\pi/3)}\frac{B_+}{3\times 2^{1/3}}, \tag{4.10}$$

where the following abbreviations have been introduced:

$$B_-=[A_-+\sqrt{A_-^2-4(\delta-V_{ab})^6}]^{1/3}, \tag{4.11}$$

$$B_+=[A_++\sqrt{A_+^2-4(\delta+V_{ab})^6}]^{1/3} \tag{4.12}$$

and

$$A_-=2(V_{ab}-\delta)^3-27(C-C_M)^2,$$

$$A_+=-2(V_{ab}+\delta)^3-27(C+C_M)^2. \tag{4.13}$$

It is easily seen that the six roots can be viewed as being the roots of two different third order polynomials. One triplet of eigenvalues corresponds to the symmetric product state, and the other triplet to the antisymmetric product state (4.2).

We found in Eq. (4.1) coupled algebraic equations governing the motion of the system. Eliminating the amplitude G_{ba} we find for G_{aa}

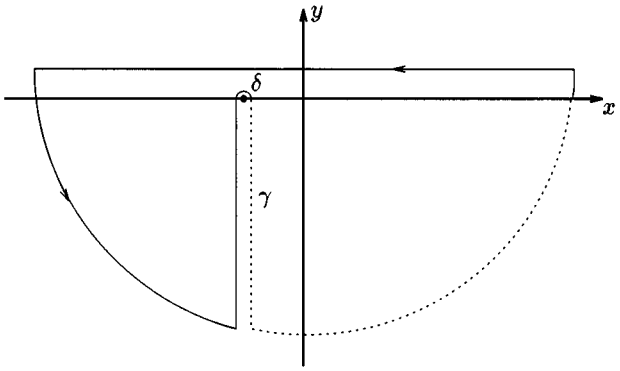

FIG. 3. The contour used to invert the amplitudes to time domain.

$$G_{aa}=\frac{z(z+\delta)+iC\sqrt{z+\delta}}{h(z)}[(z^2-V_{ba}^2)(z+\delta)+C_M^2-C^2 -2i\sqrt{z+\delta}(Cz+C_MV_{ab})] \tag{4.14}$$

and for G_{ba}

$$G_{ba}=\frac{V_{ba}(z+\delta)-iC_M\sqrt{z+\delta}}{h(z)}[(z^2-V_{ba}^2)(z+\delta)+C_M^2-C^2 -2i\sqrt{z+\delta}(Cz+C_MV_{ab})] \tag{4.15}$$

where $h(z)$ is the characteristic polynomial of Eq. (4.4). As is evident from Eqs. (4.14) and (4.15), the expressions for the amplitudes contain square root terms. This means that the amplitudes have a branch cut in the complex plane and we must therefore be very careful when performing the inversion. We take the branch cut along the negative imaginary axis thereby defining the first Riemann sheet to be $\theta \in]-\pi/2:3\pi/2[$.

We could discuss the behavior of the system in different regimes in terms of the location of the eigenvalues in the complex plane. As we mentioned above, however, there is a non-negligible contribution to the inversion integral which stems from the photonic continuum and which cannot be discussed in terms of eigenvalues. In order to see the precise behavior of the system, we therefore perform the inversion integral and investigate the system in time domain.

V. INVERSION

The inversion integral reads

$$\mathcal{U}(t)=\frac{1}{2\pi i}\int_{\infty+i\epsilon}^{-\infty+i\epsilon}dzG(z)e^{-izt} \tag{5.1}$$

where ϵ is an infinitesimal small positive quantity. To evaluate the integral, we close the contour with a semicircle in the lower half of the complex plane as depicted in Fig. 3 and use the residue theorem. When the radius of the semicircle goes to infinity, this part of the contour does not contribute. Since the functions to invert have a branch cut, we have to do a detour around the branching point. This detour, denoted γ, does contribute.

Applying the residue theorem, we find

$$\mathcal{U}_k(t)=\sum_j (z-z_j)G_{ka}(z)e^{-izt}\big|_{z=z_j} -\frac{1}{2\pi i}\int_\gamma dze^{-izt}\sqrt{z+\delta}p_k(z) \tag{5.2}$$

with $k=\{a,b\}$ and since all poles are simple. For higher-order poles, the residues are more complicated. The sum over j is a sum over all poles that do not have a positive imaginary part since those poles fall outside the integration contour. The function $p_k(z)$ introduced in the last integral is the part of the expressions for G_{aa} and G_{ba} containing the square root terms, thus

$$p_a(z)=i\frac{(z+\delta)(-Cz^2-CV_{ba}^2-2C_MV_{ba}z)+C(C_M^2-C^2)}{h(z)},$$

$$p_b(z)=-i\frac{C_M[(z^2+V_{ba}^2)(z+\delta)+C_M^2-C^2]+2V_{ba}(z+\delta)Cz}{h(z)}. \tag{5.3}$$

Let us look at the detour integral along the path γ

$$\begin{aligned}\int_\gamma dze^{-izt}\sqrt{z+\delta}p_k(z) &\overset{y=z+\delta}{=} \int_\infty^0 dye^{i(3\pi/2)}e^{-iye^{i3\pi/2}t}\\ &\times e^{i\delta t}\sqrt{e^{i3\pi/2}y}p_k(ye^{i(3\pi/2)}-\delta)\\ &+\int_0^\infty dye^{-i(\pi/2)}e^{-iye^{-i\pi/2}t}\\ &\times e^{i\delta t}\sqrt{e^{-i(\pi/2)}y}p_k(ye^{-i\pi/2}-\delta)\\ &=2ie^{i\frac{3\pi}{4}}\int_0^\infty dye^{-yt+i\delta t}\sqrt{y}p_k(-iy-\delta)\end{aligned} \tag{5.4}$$

with $k\in\{a,b\}$.

With the normalization of $2\pi i$, the detour part thus reads

$$\frac{1}{2\pi i}\int_\gamma dze^{-izt}\sqrt{z+\delta}p_k(z) =\frac{e^{i(3\pi/4)}}{\pi}\int_0^\infty dye^{-yt+i\delta t}\sqrt{y}p_k(-iy-\delta). \tag{5.5}$$

The integral cannot be computed analytically (except for certain limits) but is easily computed numerically. The influence of the integrals can, however, be found in the long time limit. In that case only the lowest order in z contributes to the integrals, and we thus find

$$\frac{1}{2\pi i}\int_\gamma dz e^{-izt}\sqrt{z+\delta}p_a(z)\simeq\frac{e^{i(3\pi/4)}}{\pi}\int_0^\infty dy e^{-yt+i\delta t}\sqrt{y}p_a(0)$$
$$=\frac{e^{i(3\pi/4)+i\delta t}}{\pi}p_a(0)\frac{\Gamma(3/2)}{t^{3/2}}. \tag{5.6}$$

In the long time limit, the detour integral thus contributes as $t^{-3/2}$. A similar behavior is found for the other detour integral.

The prefactor $p_a(0)$ in Eq. (5.6) determines the influence of the detour integral on the total wave function. By examining the expression for $p_k(z)$, one finds $p_k(0)\propto\delta^{-1}$ for large detunings. The influence of the detour integral therefore becomes negligible when the atomic transition frequency is detuned far from the band-gap edge in which case the atomic evolution becomes exponential (positive detuning) or the decay is inhibited (negative detuning).

The behavior of the system resembles the departure from exponential decay for an atom in free space due to corrections to the pole approximation [14]. We recall, however, that in our problem the photon continuum is strongly modified compared to the free space case, and the pole-approximation does not provide a valid starting point for our calculation.

VI. WAVE FUNCTIONS IN TIME DOMAIN

Having established the influence of the detour integral, we investigate the system in different limits in the time domain.

A. One atom

If the interatomic separation is very large, we have $C_M\sim V_{ab}\sim 0$ and the problem reduces to the one-atom problem already treated in the literature [3,4]. In that case the characteristic polynomial (4.4) simplifies to

$$0=[z^2(z+\delta)+C^2]^2, \tag{6.1}$$

which seems to indicate that this one-atom system has three poles that are all of order 2. The expression for G_{aa} does, however, simplify and we find

$$G_{aa}=\frac{z(z+\delta)-i\sqrt{z+\delta}C}{z^2(z+\delta)+C^2}, \tag{6.2}$$

which is the expression also derived by John and Quang [3]. This expression has three poles, of which only two contribute since the third pole has a positive imaginary part and thus falls outside the inversion contour. Of the two remaining poles, one has an imaginary part and thus gives rise to a transient, dissipative dynamics, whereas the second pole is purely real and thus corresponds to a stable, nondecaying state of the system. In the transient regime, both poles will contribute to the dynamics which gives rise to beating, which is indeed a rather unusual phenomenon in spontaneous decay.

For an atomic transition frequency at the band edge ($\delta=0$), the roots are

$$z_1=-C^{2/3}, \tag{6.3}$$

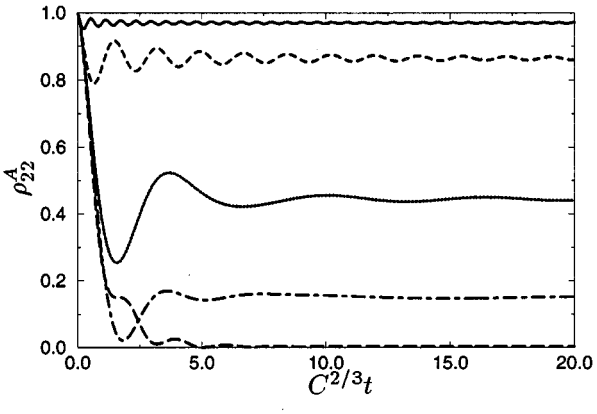

FIG. 4. The time evolution of the excited state population as a function of time for different detunings: $\delta=-10C^{2/3}$ (solid line), $\delta=-3C^{2/3}$ (dashed line), $\delta=0$ (dotted line), $\delta=C^{2/3}$ (dash-dotted line), and $\delta=3C^{2/3}$ (long-dashed line).

$$z_2=e^{i(\pi/3)}C^{2/3},$$

$$z_3=e^{-i(\pi/3)}C^{2/3}.$$

In the long time limit, only the real root contributes and the atomic population is then given by

$$|\mathcal{U}_{aa}(t)|^2=\left|\frac{z_1^2-iC\sqrt{z_1}}{(z_1-z_2)(z_1-z_3)}\right|^2=\frac{4}{9}, \tag{6.4}$$

which means that a considerable part of the population is bound on the atom in the long time limit. This is what has been referred to as a ''bound photon-atom state'' in the literature [3]. For atomic transition frequencies in the gap, the population trapping can be close to 1 as is evident from Fig. 4, where we have plotted the atomic population as a function of time for different detunings with respect to the band-gap edge.

Spontaneous emission is taking place on a fast time scale roughly given by $C^{-2/3}$ and in this transient regime, part of the atomic population is lost. On a longer time scale, the population remains almost constant but we see a slight oscillation which stems from the beating between the stable, nondecaying state and the detour integral. Physically, this effect stems from the emitted photon which is reflected in the dielectric host and thus oscillates back and reexcites the atom. Even for atomic transition frequencies outside the gap ($\delta>0$), we find a significant population trapping, as has been noted in the literature [3,4].

B. Two atoms at the band edge ($\delta=0$)

At the band edge $\delta=0$ and for negligible dipole-dipole coupling $V_{ab}\simeq 0$, the roots of the characteristic polynomial are the following:

$$z_1=e^{i\pi/3}(C+C_M)^{2/3}, \tag{6.5}$$

$$z_2=e^{-i\pi/3}(C+C_M)^{2/3}, \tag{6.6}$$

$$z_3=-(C+C_M)^{2/3}, \tag{6.7}$$

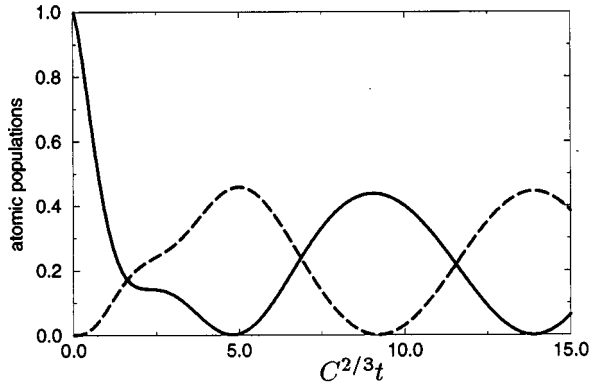

FIG. 5. The time evolution of the excited state populations as a function of time for atomic transition frequencies at the band edge ($\delta=0$). The solid line is the population of the initially excited atom A and the dashed line is for atom B. $C_M/C=\frac{1}{2}$, $V_{ab}=0$.

$$z_4=e^{i\pi/3}(C-C_M)^{2/3}, \tag{6.8}$$

$$z_5=e^{-i\pi/3}(C-C_M)^{2/3}, \tag{6.9}$$

$$z_6=-(C-C_M)^{2/3}. \tag{6.10}$$

Two of these roots are real, namely, $z=-(C+C_M)^{2/3}$ and $z=-(C-C_M)^{2/3}$, and by inserting these in the characteristic equation (4.3), it is easily confirmed that these roots are also roots in the original polynomial. That the roots are real means that they correspond to stable, nondecaying states of the coupled system. The existence of two such stable states implies that the system has no steady state in the conventional sense of the word, since in the long time limit, the system will beat between these two nondecaying states. On the other hand, if the system is viewed in the basis of the symmetric and antisymmetric product states, it is found to have a steady state.

Of the four remaining roots, two will not contribute since they have a positive imaginary part and thus fall outside the integration contour and the two remaining roots will give rise to a transient, damped behavior.

Now, one of the real poles corresponding to a stable state is actually the eigenvalue of the symmetric product state. We thus find the surprising result that the symmetric product state which in free space is super-radiant in the photonic band gap can be a stable nondecaying state. In Fig. 5 we have plotted the atomic populations as a function of time. From the figure, we identify an initial transient regime in which part of the population is lost. On a longer time scale, the remaining population is exchanged between the atoms in an oscillatory, nondissipative manner. This is also a rather surprising result: In the study of atoms coupled to cavities, we typically see beating (Rabi oscillations) when the Rabi frequency exceeds the decay width and the Rabi oscillation is then a transient phenomena, which is eventually damped out. In the present problem, dissipation only acts in a transient regime, after which it is effectively turned off and then only the coherent oscillation of the remaining excitation between the two atoms persists. Physically, this part of the excitation is protected against dissipation, since it corresponds to a photon with energy in the gap, tunneling between the two atoms.

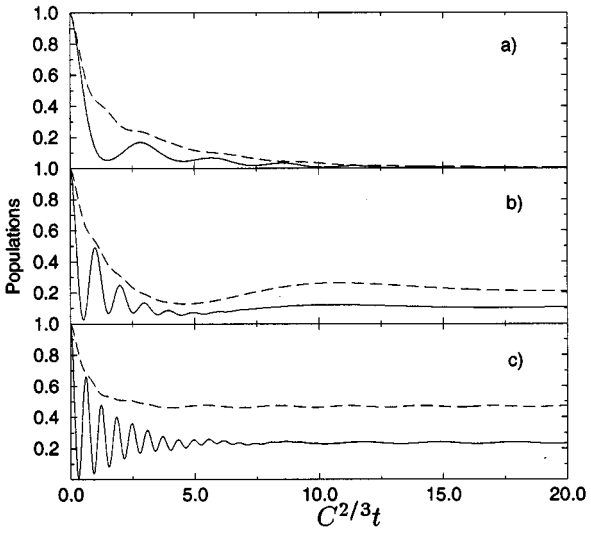

FIG. 6. The excited state populations as a function of time for $\delta=3$, $C=1$, $C_M=0.8$ and different values of V_{ab}. The solid line is the population in the excited state of atom A. The dashed line is the sum of the populations in the excited states of atom A and B. (a) $V_{ab}=1$. (b) $V_{ab}=3$. (c) $V_{ab}=5$.

C. Small interatomic separation

When the interatomic separation becomes very small, i.e., $R\ll\lambda$, the real part of the dipole-dipole interaction (V_{ab}) becomes the dominant part of the interaction. We investigate this regime for different detunings.

In Fig. 6 we plot the population in the excited state of the initially excited atom A and the total population of atom A and B as a function of time for different values of V_{ab} with $\delta=3$. With this choice of parameters, the atomic transition frequencies are tuned outside the gap into the allowed part of the spectrum. For a relatively weak RDDI ($V_{ab}=1$), the atomic population is lost in the long time limit as is evident from the figure. For a slightly stronger RDDI ($V_{ab}=3$), the coupling between the two atoms is now comparable to the detuning from the band-gap edge and the splitting of the atomic levels due to the coupling is hence strong enough to move part of the atomic level into the gap where it is protected from dissipation. We therefore find a non-negligible population trapping for this choice of parameters. This becomes even more apparent for an even stronger coupling ($V_{ab}=5$), in which case close to 50% of the initial excitation remains bound on the two atoms in the long time limit.

The reverse case is illustrated in Fig. 7, where again the atomic population on atom A and the sum of the atomic populations are plotted for $\delta=-3$ and various values of V_{ab}. For a relatively weak RDDI ($V_{ab}=1$), there is a significant population trapping in the long time limit. As the RDDI is becoming comparable to the detuning from the band-gap edge, the population trapping is decreased since the level splitting is now large enough to move part of the atomic levels into the allowed part of the spectrum.

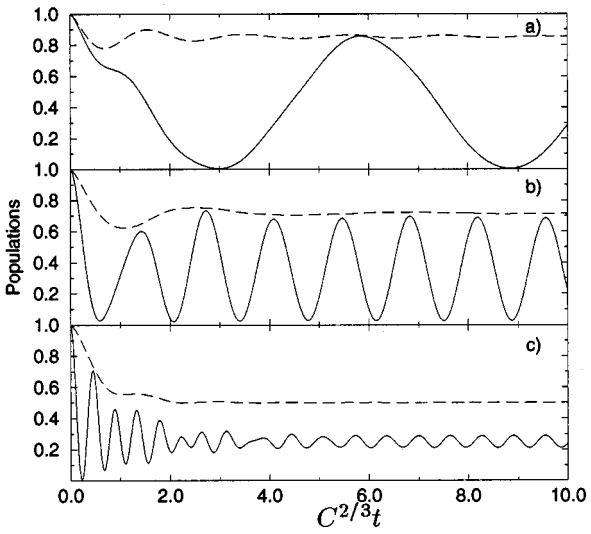

FIG. 7. The excited state populations as a function of time for $\delta=-3$, $C=1$, $C_M=0.8$, and different values of V_{ab}. The solid line is the population in the excited state of atom A. The dashed line is the sum of the populations in the excited states of atom A and B. (a) $V_{ab}=1$, (b) $V_{ab}=3$, and (c) $V_{ab}=7$.

VII. PHOTONIC POPULATION DISTRIBUTION

In the literature, different quantities have been employed as a measure of the spectrum [15]. For an atom in free space, the spectrum is the distribution of population in the continuum modes in the long time limit. In the present case, however, an initially excited atom with a transition frequency close to the edge of the gap with a certain probability evolves into a photon-atom bound state which is a superposition of atomic excited state in the presence of no photon and atomic ground state with a superposition of one-photon states. The superposition of photonic states yields a wave packet in real space which is well localized around the atom. A detector located outside the large crystal does not detect the localized photonic wave packet but only the fluorescent light lost in the initial transient regime of the atomic evolution. The distribution of population in the photonic continuum does therefore not coincide with the spectrum we would measure with a detector located outside the crystal. Kofman and co-workers have investigated the spectrum of one atom in a photonic band-gap material [4].

In this section we investigate the distribution of population in the continuum in the long time limit.

A. One atom

The one-photon part of the field in the time domain is given by

$$|\psi\rangle=\sum_{\mathbf{k}l}\mathcal{U}_{ca}(t)|\mathbf{k}l\rangle, \tag{7.1}$$

where the summation is over all continuum states and $\mathcal{U}_{ca}$ is the amplitude for the continuum mode c with frequency $\omega_c=\omega_a+\Delta$, obtained by inverting the expression

$$G_{ca}=\frac{V_{ca}G_{aa}}{z-\Delta}, \tag{7.2}$$

where G_{aa} is the one-atom amplitude given by Eq. (6.2).

In the long time limit, only the roots with no imaginary (dissipative) part contribute to the dynamics in time domain of the continuum mode. Assuming that the atomic transition frequency is at the band-gap edge ($\delta=0$), there are two poles contributing: One is the free evolution of the mode at frequency ω and the other pole at $-C^{2/3}$ stems from the nondecaying photon-atom bound state. In this case, the population in the mode is

$$|\mathcal{U}_{ca}(t)|^2=\frac{|V_{ca}|^2}{(\Delta+C^{2/3})^2}\left[\frac{\Delta^4+C^2\Delta}{(\Delta^2+C^{4/3}-\Delta C^{2/3})^2}+\frac{4}{9}-\frac{4}{3}\frac{\Delta^2}{\Delta^2+C^{4/3}-\Delta C^{2/3}}\cos(\Delta t+C^{2/3}t)+\frac{4}{3}\frac{C\sqrt{\Delta}}{\Delta^2+C^{4/3}-\Delta C^{2/3}}\sin(\Delta t+C^{2/3}t)\right]. \tag{7.3}$$

Equation (7.3) contains an implicit dependence on the orientation of the atomic dipole in space. We perform an integration of Eq. (7.3) over the angular part. Furthermore, we perform a time average over the period $2\pi/(\Delta+C^{2/3})$ in order to eliminate the time-dependent terms.

In the long time limit, the frequency distribution is therefore given by the angular integrated, stationary terms of Eq. (7.3)

$$S(\omega)=\rho(\omega)\sum_{l=1,2}\int d\Omega|\mathcal{U}_{ca}|^2=\frac{\Theta(\omega-\omega_e)}{\pi\sqrt{\omega-\omega_e}}\frac{C}{(\Delta+C^{2/3})^2}\left[\frac{\Delta^4+C^2\Delta}{(\Delta^2+C^{4/3}-\Delta C^{2/3})^2}+\frac{4}{9}\right], \tag{7.4}$$

where $\omega=\omega_a+\Delta=\omega_e+\Delta$ since $\delta=0$ and the density of states $\rho(\omega)$ is given by Eq. (3.19). Equation (7.4) does indeed yield a rather unusual distribution of population quite different from the usual Lorentzian form obtained for a two-level atom in free space, as can also be seen from Fig. 8, where we have plotted the frequency distribution as a function of ω.

The coupled system consisting of ''atom+reservoir'' has a pole at $\exp(-i\pi/3)C^{2/3}$ and we would thus expect the population distribution to have a peak at $\frac{1}{2}C^{2/3}$. The density of modes does, however, strongly suppress radiation at this wavelength and instead the photon emission close to the band-gap edge ($\Delta\approx 0$) is strongly amplified.

We calculate the population in the continuum modes in the long time limit, which is given by

$$\int_0^\infty d\omega S(\omega)=\frac{5}{9}. \tag{7.5}$$

To obtain this result, the integral has been performed numerically. In the long time limit, we therefore find that the

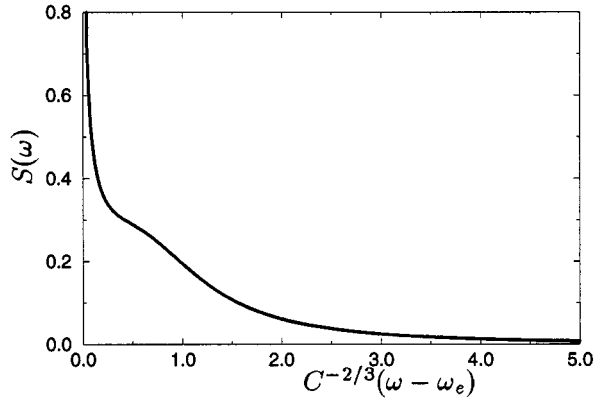

FIG. 8. The photonic population distribution for one atom in a photonic band gap with transition frequency at the band-gap edge ($\delta=0$).

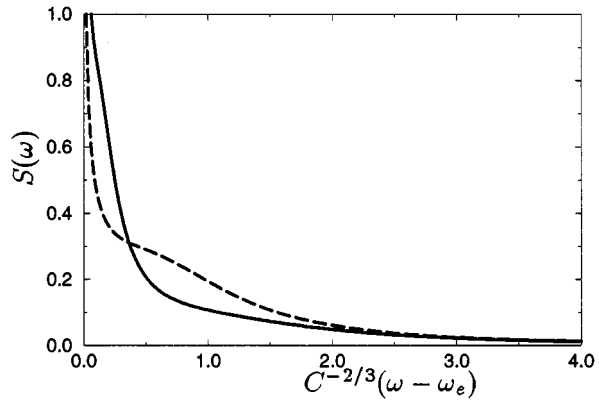

FIG. 9. The photonic population distribution for two atoms in a photonic band gap with transition frequencies at the band-gap edge ($\delta=0$) and $V_{ab}=0$. The solid line is for $C_M/C=0.9$ and the long-dashed line is for $C_M/C=0.1$.

atomic excited state population given by Eq. (6.4) and the population in the photonic continuum add up to 1, as should be the case.

B. Two atoms

When the couplings between the two atoms cannot be neglected, the general expression for the continuum amplitude in frequency domain reads

$$G_{ca}=\frac{1}{z-\omega_c}[V_{ca}G_{aa}+V_{cb}G_{ba}]. \tag{7.6}$$

Let us consider the simpler case of $V_{ab}=\delta=0$. The roots of the system are then given by Eqs. (6.5)–(6.10) and the expression for the continuum amplitude reads

$$G_{ca}=\frac{1}{z-\omega_c}\frac{1}{h(z)}[V_{ca}(z^2+iC\sqrt{z})-iV_{cb}C_M\sqrt{z}] \times[z^3+C_M^2-C^2-2iC\sqrt{z}z], \tag{7.7}$$

while the stable roots of the system are given by Eqs. (6.7) and (6.10). In the long time limit, these roots and the root $z=\omega$ contribute. As before, we transform the amplitude to the time domain keeping only the contribution from real roots, taking absolute square and leaving out terms depending on frequency. In the end, we obtain for the angular integrated continuum population

$$S(\omega)=\rho(\omega)\sum_{l=1,2}\int d\Omega|\mathcal{U}_{ca}(t)|^2=\frac{\Theta(\omega-\omega_e)}{\pi\sqrt{\omega-\omega_e}}\frac{C\Delta}{h(\Delta)^2} \times[\Delta^3+C^2-C_M^2][(\Delta^3+C_M^2-C^2)^2+4\Delta^3C^2] + \frac{\Theta(\omega-\omega_e)}{\pi\sqrt{\omega-\omega_e}}\frac{32C^2C_M^2}{9\tilde{h}^2}\left[\frac{C-C_M}{[(C-C_M)^{2/3}+\Delta]^2} + \frac{C+C_M}{[(C+C_M)^{2/3}+\Delta]^2}\right], \tag{7.8}$$

where we have defined

$$\tilde{h}=[(C-C_M)^{4/3}+(C+C_M)^{4/3}-(C^2-C_M^2)^{2/3}] \times[(C+C_M)^{2/3}-(C-C_M)^{2/3}]. \tag{7.9}$$

The population distribution (7.8) has been plotted in Fig. 9. From the figure, we find that the population distribution has a ''shoulder'' which vanishes when $C\sim C_M$. The reason for this becomes apparent by investigating the eigenvalues of the coupled system. The coupled system fluoresces at the energies $\frac{1}{2}(C-C_M)^{2/3}$ and $\frac{1}{2}(C+C_M)^{2/3}$. The shoulder in the population distribution thus stems from the fluorescence at the energy $\frac{1}{2}(C-C_M)^{2/3}$, which coincides with the band-gap edge when $C\sim C_M$, in which case the shoulder disappears. As in the case of one atom, we have, by numerical integration of the population distribution over ω, made sure that the population in the continuum modes and the atomic excited state population add up to 1.

VIII. SUMMARY

In this paper we have presented a model calculation for two atoms with transition frequencies near the edge of a photonic band gap and interacting through the narrow band of strongly coupled modes. We addressed the problem using the resolvent operator formalism by means of which the wave functions of the system are obtained in Laplace space. Eliminating the field mode amplitudes from the equations of motion, we obtained two coupled, algebraic equations for the amplitudes of the two atoms coupled through second-order expressions involving summations over the continuum states. One of these couplings is the RDDI between the two neighboring atoms. We presented an analytical calculation of the RDDI and showed that it agrees very well with a numerical integration of the RDDI using the exact dispersion relation for the dielectric host. With the analytical expressions for the couplings, the set of equations for the two atoms was solved and we investigated the amplitudes of the two atoms in the time domain. Although the atoms are coupled to a dissipative environment, we found population trapping and beating in

the long time limit for a wide range of parameters.

We have also calculated the photonic population distributions for one and two atoms, respectively, and found that the location of the peaks of the distributions is mainly determined by the mode structure and not as is usually the case, by the location of the poles of the coupled system in the complex plane. Furthermore, we found, not surprisingly, that the mode structure acts as a frequency filter and effectively cuts off frequencies in the photon distribution below the band edge.

[1] E. Yablonovitch, Phys. Rev. Lett. **58**, 2059 (1987).
[2] S. John, Phys. Rev. Lett. **58**, 2486 (1987).
[3] S. John and T. Quang, Phys. Rev. A **50**, 1764 (1994).
[4] A. Kofman, G. Kurizki, and B. Sherman, J. Mod. Opt. **41**, 353 (1994).
[5] R. H. Dicke, Phys. Rev. **93**, 99 (1954).
[6] M. Gross and S. Haroche, Phys. Rep. **93**, 301 (1982).
[7] G. Kurizki, A. G. Kofman, and V. Yudson, Phys. Rev. A **53**, R35 (1996), and references therein.
[8] S. Bay, P. Lambropoulos, and K. Mølmer, Opt. Commun. **132**, 257 (1996).
[9] S. John and T. Quang, Phys. Rev. A **52**, 4083 (1995).
[10] R. G. DeVoe and R. G. Brewer, Phys. Rev. Lett. **76**, 2049 (1996).
[11] C. Cohen-Tannoudji, J. Dupont-Roc, and G. Grynberg, *Atom-Photon Interactions* (Wiley, New York, 1992).
[12] S. John and J. Wang, Phys. Rev. B **43**, 12 772 (1991).
[13] G.-I. Kweon and N. M. Lawandy, J. Mod. Opt. **41**, 311 (1994).
[14] M. L. Goldberger and K. M. Watson, *Collision Theory* (Wiley, New York, 1964).
[15] J. H. Eberly and K. Wodkiewicz, J. Opt. Soc. Am. **67**, 1252 (1977).